J. exp. Biol. 143, 245–265 (1989)
Printed in Great Britain © The Company of Biologists Limited 1989

SIZE LIMITS IN ESCAPE LOCOMOTION OF CARRIDEAN SHRIMP

BY THOMAS L. DANIEL AND EDGAR MEYHÖFER

Department of Zoology, NJ-15, University of Washington, Seattle, WA 98195, USA

Accepted 7 December 1988

Summary

Escape locomotion of the common dock shrimp, *Pandalus danae* Stimpson, is the result of a rapid flexion of the abdomen that lasts approximately 30 ms. The hydrodynamic forces that result from this motion lead to body accelerations in excess of $100\,m\,s^{-2}$ and body rotations of about 75°. We examined the mechanics and kinematics of this mode of locomotion with both experimental and theoretical approaches. Using a system of differential equations that rely on conservation of both linear and angular momenta, we develop predictions for body movements, thrust forces and muscle stresses associated with escape locomotion. The predicted movements of the body agree to within 10 % with data from high-speed ciné-photography for body translations and rotations. The thrust from rapid tail flexion is dominated by accelerational forces and by the force required to squeeze fluid out of the gap created by the cephalothorax and the abdomen at the end of tail flexion. This squeeze force overwhelms any propulsive drag forces that arise from the tail-flip.

Using the theoretical analysis, we identify two additional features about unsteady, rotational aquatic locomotion. First, as either the relative length of the propulsive appendage increases or the absolute body size increases, rotational motions become disproportionately greater than translational motions, and escape performance decays. Second, if muscle stresses developed during escape cannot exceed the maximum isometric stress, there is a unique body length (6 cm) that maximizes the distance travelled during the escape event.

Introduction

Most analyses of animal locomotion, and animal swimming in particular, assume two important aspects of motility: (1) steady-state locomotion, in which the mean speed of the body remains constant in time, and (2) rectilinear movements, in which the body travels along a straight path (see for example Lighthill, 1975; Wu, 1971*a*,*b*,*c*). Under these conditions, experiments and theoretical analyses are directed towards understanding the implications of appendage kinematics, body form or body size for some measure of performance such as

Key words: shrimp, escape, hydrodynamics, muscle stress, aquatic locomotion.

speed, cost of transport or efficiency (for reviews see Daniel & Webb, 1987; Webb, 1984; Herreid & Fourtner, 1981; Wu *et al.* 1975). Indeed, a number of important limitations to the behaviour and morphology of swimming animals have been illuminated by such approaches. For example, the significant energy savings in burst-and-coast locomotion of fish (Weihs, 1974, 1980), the existence of optimal body morphologies of fish (Wu, 1971*b*), the implications of body form for locomotor performance of fish (Webb, 1984) and optimum motions of flying and swimming animals (Yates, 1986) have all followed from careful theoretical analyses of swimming that relate to either one or both of the above criteria.

Despite the wealth of information we have gained from these approaches, there are still some very large gaps in our knowledge of constraints (physical and physiological) on the behaviour and morphology of swimming animals. Chief among these gaps is our understanding of the limits imposed on animals that undergo large accelerational or rotational motions in escape from predation or attack on prey. For such cases, the traditional ideas of energy minimization or speed maximization for steady-state rectilinear motion no longer apply (Weihs & Webb, 1983). Instead, we must seek some other measures of performance, such as absolute acceleration or the distance travelled in a short time, that reflect this possibly infrequently used, yet selectively important, mode of locomotion. The idea of constraints on the size, shape or behaviour of animals undergoing escape manoeuvres has never been clearly defined. If selection for high performance in such situations is particularly strong, we may expect the morphology of many animals to reflect not the common steady-state mode of movement, but the infrequently used, unsteady, accelerational mode.

This paper focuses on such contraints to accelerational locomotion for one group of organisms, carridean shrimps. These animals utilize a powerful tail-flip in escape from predation. They provide a unique opportunity to examine fully the kinematic and morphological determinants of the hydrodynamic forces acting on a swimming animal. Unlike the theoretical developments for fish locomotion, in which our knowledge of resistive forces is still incomplete (Wu, 1975), the high accelerations of shrimps and their rigid bodies lead to a system that is, for all practical purposes, entirely dominated by inertial forces for which the fluid reactions are well known (Daniel, 1984). Armed with relatively simple theories and experiments, this paper addresses two questions. What are the mechanics of thrust production for the carridean tail-flip and is there a size limit to this mode of locomotion?

Theoretical basis

Fundamental to our understanding of limits to body size in escape locomotion is a careful analysis of the hydrodynamic forces that are produced by the propulsor and those that resist the motion of the body. There are only a handful of studies in which the hydrodynamics for accelerational locomotion have been analysed (Weihs, 1972; Wu, 1971*b*; Webb, 1976, 1979, 1983; Daniel, 1984, 1985; Daniel &

Webb, 1987). In all these cases, accelerations of a body lead to large hydrodynamic reactions known as added-mass forces (Batchelor, 1967), as well as the more commonly recognized drag forces. For an animal accelerating in an arbitrary direction, the x-component of the forces that resist the motion of the body balances the x-component of the thrust [$T_x(t)$] produced. Thus:

$$T_x(t) = 0{\cdot}5\rho S C_{dx} U_x^2 + \alpha_x \rho V dU_x/dt + m dU_x/dt\,, \quad (1)$$

$$\text{thrust} = \text{drag} + \text{added-mass force} + \text{body inertial force}\,,$$

where ρ is the density of water; C_{dx} is the drag coefficient for motion in the x-direction; U_x is the instantaneous velocity of the body in the x-direction; α_x is the added-mass coefficient that depends upon the orientation of the body in the x-direction; S, V and m are, respectively, the surface area, volume and mass of the body; and t is time. Thrust is thus balanced at any instant in time by the fluid drag and added-mass force as well as the body inertia. A similar form of equation 1 gives the y-component of the force balance:

$$T_y(t) = 0{\cdot}5\rho S C_{dy} U_y^2 + \alpha_y \rho V dU_y/dt + m dU_y/dt\,, \quad (2)$$

where the subscript y corresponds to motions and coefficients for movement in the y-direction.

In addition to these translational components of force, we must also consider those rotational components that affect the motion of the body. Thus, while satisfying a linear momentum balance for both x- and y-components of motion, we must also include conservation of angular momentum. For this condition, the moments generated by an impulsive flip of the tail [M(t)] are balanced by the moments that resist rotation of the body. These latter moments are the sum of the steady (drag-related) and unsteady (added-mass related) hydrodynamic reactions to body rotation, as well as the rotational inertia of the body. Thus:

$$M(t) = C_{dr}\rho S\omega^2 + \gamma V\rho(d\omega/dt) + I(d\omega/dt)\,, \quad (3)$$

where C_{dr} is the rotational drag coefficient (not dimensionless) for the body of the shrimp, ω is the angular velocity of the body, γ is the added-mass coefficient for rotational acceleration (see Brennen, 1982), and I is the rotational inertia of the body, here assumed to be a prolate spheroid (Brennen, 1982):

$$I = 4\rho\pi ab^2(a^2 + b^2)/15\,, \quad (4)$$

where a and b are, respectively, the semi-major and semi-minor axes of the spheroid. Unlike equation 1, which is a linear momentum balance, equation 3 has two size-dependent coefficients, C_{dr} and γ.

The left-hand sides of equations 1, 2 and 3, symbolized as $T_x(t)$, $T_y(t)$ and $M(t)$, represent thrust forces that arise from three physical mechanisms: thrust produced by drag, added-mass forces, and the squeeze of fluid between the thorax and the abdomen/tail complex. The former two forces are simply the reaction in the fluid to motion of the tail. The latter force [$T_s(t)$] arises from the pressure created as fluid is squeezed out of the space between the abdomen and cephalothorax, much

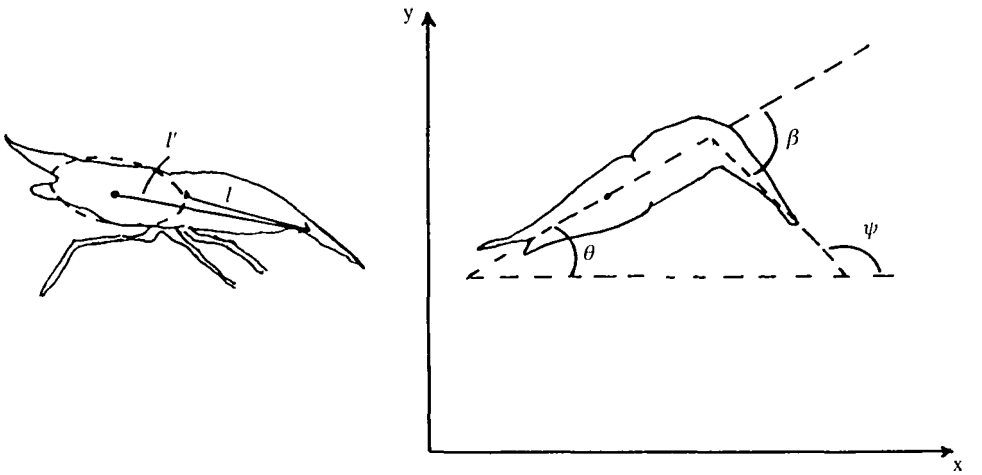

Fig. 1. A diagram showing the various angles and linear dimensions used in the equations of motion. The distance along the tail is l and the distance from the centre of gravity to any point on the tail is l'. The angle of the body with respect to the horizon (θ) as well as the angle of the tail with respect to the body (β) and the angle of the tail with respect to the horizon (ψ) are shown in the right-hand diagram.

like the jet reaction mechanism of medusae and salps (Daniel, 1983, 1985; Bone & Trueman, 1983). In equation form the thrust developed is:

$$T_x(t) = \left[0{\cdot}5\rho \int_0^L wC_{dl}u_n^2\, dl + \rho \int_0^L \alpha_t A\, (du_n/dt)dl + T_s(t)\right] \sin(\psi), \quad (5)$$

where L is the length of the tail, w is the width of the tail (which may vary with length), C_{dl} is the sectional drag coefficient of the tail, u_n is the fluid velocity normal to the tail, α_t is the sectional added-mass coefficient of the tail, A is the local cross-sectional area of the tail, and ψ is the angle subtended between the tail and the horizon. This equation states that the thrust is a function of the drag and added-mass forces acting on the tail plus the force generated by the squeeze of water between the tail and cephalothorax at the end of the tail-flip cycle. For brevity, we refer to this latter force as the squeeze force (see below). The normal velocity of the tail with respect to the fluid is:

$$u_n(l,t) = l d\beta/dt - U_x\sin(\beta) - U_y\cos(\beta) - l'(d\theta/dt)\cos(\beta - \theta), \quad (6)$$

where l is the position along the tail, l' is the distance of the centre of gravity from any point on the tail, β is the angle subtended by the tail and cephalothorax, U_x and U_y are, as before, the x- and y-components of the body velocity, and θ is the angle of the body with respect to the horizon (see Fig. 1).

Equation 3 contains two rather standard fluid dynamic forces, drag and acceleration reaction (added-mass forces), which have been applied to numerous studies of aquatic swimmers (e.g. Blake, 1981, 1983; Webb, 1979; Nachtigall, 1980; Daniel, 1984; Daniel & Webb, 1987). These analyses treat propulsive appendages

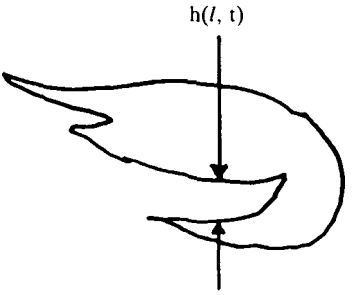

Fig. 2. The parameter $h(l, t)$ is the width of the gap created by the abdomen and cephalothorax.

such as the abdomen of the shrimp, as oars swimming through the water. Unfortunately, all these studies have neglected the fluid-dynamic interaction between the body and the propulsor. As the tail of the shrimp closes against the cephalothorax, it must squeeze water in a way that is analogous to a jet reaction mechanism found in medusae and squid (Daniel, 1983,1985; O'Dor, 1988; Bone & Trueman, 1983) or the 'fling' mechanism created by the closure of two wings in hovering insects (Ellington, 1984; Lighthill, 1975). This squeeze generates a thrust force that is estimated with a modification of Brennen's (1982) analysis of closing plates, where the sectional force depends on the speed and acceleration of the tail with respect to the body:

$$T_s(t) = (2\rho/3) \int_0^L \frac{w^3}{h} \left[\frac{2}{h} \left(\frac{\partial h}{\partial t} \right)^2 - \frac{**\partial^2 h}{\partial t^2} \right] dl, \tag{7}$$

where w is the local width of the tail and h is the local distance between the tail and cephalothorax (see Fig. 2).

Thrust generated by this scheme (equation 7) is at least equal to the total thrust generated by drag and acceleration forces. This novel mechanism of thrust production has not been considered in any previous analyses of animal swimming in which there is closure of a propulsor against the body, as might be the case for fish which swim with pectoral fins (Blake, 1981, 1983) or aquatic insects (Nachtigall, 1980).

With analytical expressions for the x- and y-components of thrust and reactive and resistive forces on the body, as well as the moments produced by the tail and those that resist the motion of the body, a system of differential equations is defined. These are, with the derivatives of translational and rotational speeds as the dependent variables:

$$\Sigma F_x = m(dU_x/dt) \tag{8a}$$

$$\Sigma F_y = m(dU_y/dt) \tag{8b}$$

$$\Sigma M = I(d\omega/dt), \tag{8c}$$

where F_x and F_y are the x- and y-components of propulsive and reactive forces and M is the total moment acting about the centre of gravity of the animal.

Since equations 8a–c yield a system of simultaneous second-order differential equations with nonlinear coefficients, a solution can only be achieved numerically. The numerical method used in this study is basically a modified fourth-order Runge–Kutta scheme with an Adams–Bashforth predictor–corrector scheme (Wylie, 1975; Mathews, 1987). By this method, the instantaneous x- and y-coordinates of the body and its instantaneous angle are computed in a step-wise manner as a solution to the system of differential equations. Each time step in the simulation corresponds to 0·1 ms, yielding approximately 300 point solutions to the system.

Materials and methods

Animals

Specimens of *Pandalus danae* were collected with dip nets off the pilings and supports around the docks of the Friday Harbor Laboratories at the University of Washington. They were transferred to holding tanks with with flow-through sea water and maintained at 12°C.

Morphology

For each animal, the following morphological features were measured: (1) mass was measured with a digital balance (Sartorius); (2) volume of individuals was determined by fluid displacement; (3) the relative dimensions of the abdomen, carapace and rostrum, and the area of the uropod–telson complex were measured with calipers; (4) using a dissecting microscope equipped with an ocular micrometer, the maximum cross-sectional area of abdominal flexors and extensors was measured from cross-sections through the second abdominal segment.

Movements

Individuals, placed in a large glass aquarium (approx. 190 l), were filmed with a high-speed camera (Locam) at 200 or 500 frames s^{-1}. To initiate the tail-flip response, the antenna of an individual was gently squeezed by the investigator. Just prior to this provoking process, the camera was triggered by a foot pedal so that the entire escape sequence could be captured on film. Only those film sequences in which the animal travelled parallel to the plane of focus were used in the analysis. This potential problem of parallax was avoided by using film sequences in which the image of the shadow cast by the animal on the rear wall of the aquarium remained a constant distance from the image of the animal itself.

A stop-motion projector (NAC) was used for sequential frame analysis. From the projected image of each frame three distinct landmarks on the animal were digitized: (1) the tip of the rostrum, (2) the junction between the cephalothorax and the abdomen, and (3) the tip of the uropods. From these data and a known duration between consecutive frames, the x- and y-components of the displac

ment, the angle of the body and the duration of the tail-flip were computed. Numerical differentiation of these data provided, in turn, the linear and angular speeds and accelerations of the body.

Hydrodynamic coefficients

Models of two sizes of *Pandalus danae* were used for measurements of drag and added-mass coefficients. The models were prepared by embedding, in silicon sealant (Dow Corning), preserved individuals with their abdomen in the fully flexed position. These negative moulds were then injected with a urethane foam to provide a light and rigid replica of the animal. Such low-mass models are necessary for measurements of added-mass coefficients and are suitable for measurements of drag coefficients.

Drag coefficients were measured with a method similar to that used by Denny *et al.* (1985). The models were attached to a strain-gauge force platform *via* a rigid aluminium sting and suspended in a flow tank. The drag force was measured for four (0·4, 0·5, 0·7 and 1·0 $m\,s^{-1}$) fluid speeds on all models. Dividing the drag by the quantity $0{\cdot}5\rho Su^2$, where S is the cross-sectional area of the animal in the direction of movement ($S = \pi ab$), yielded the drag coefficient. The force acting on these models was initially recorded as a voltage output from the platform and later converted to force by using a calibration curve. Calibration of the force platform was accomplished by suspending known weights from the tip of the sting and recording the resulting voltage. Force measurements made in this way were reliable to the nearest 0·5 mN. Rotational drag coefficients were taken to be equal to the translational drag coefficient times the major axis of the animal.

Added-mass coefficients were measured according to the method outlined by Daniel (1985) and Denny (1982), whereby the force required to accelerate a model through stationary fluid can be measured. Models were accelerated in a long trough of water with their long axes parallel to the direction of motion. The acceleration of the models was measured with an accelerometer (Entran Devices, model EGA-125) mounted adjacent to the models. The force resulting from this acceleration was measured with a strain-gauge force platform. In all cases, the force required to accelerate the platform without models was subtracted from the total force measurements.

For the first few diameters of travel, the total force required to accelerate a model is entirely dominated by its inertia and added-mass. Thus, the coefficient was calculated from the following equation:

$$\alpha = (F - mdu/dt)/(m_d du/dt), \tag{9}$$

where F is the measured force, m is the mass of the model, and m_d is the mass of displaced fluid. The mass of displaced fluid was determined by measuring, with a bottom-loading pan balance, the mass of submerged models. The difference between weight in air and submerged weight yields the mass of displaced fluid (Daniel, 1985). The added-mass coefficient for rotational acceleration was taken from Brennen's (1982) analysis of rotating prolate ellipsoids. This, in addition to

translational added-mass coefficients, may be predicted from the following (Brennen, 1982):

$$A_o = \frac{1-e^2}{e^3}\left[\ln\left(\frac{1+e}{1-e}\right) - 2e\right] \tag{10a}$$

$$B_o = \frac{1-e^2}{e^3}\left[\frac{e}{1-e^2} - \frac{1}{2}\ln\left(\frac{1+e}{1-e}\right)\right] \tag{10b}$$

$$\alpha = A_o/(2 - A_o) \tag{10c}$$

$$\gamma = \frac{(a^2-b^2)^2\,(B_o - A_o)}{(a^2+b^2)[2(a^2-b^2) - (a^2+b^2)(B_o - A_o)]}, \tag{10d}$$

where e is the eccentricity and a and b are, as above, the semi-major and semi-minor axes of the ellipsoid.

Results

Morphology

Fig. 3 shows that over about one order of magnitude, size variation is isometric. This is particularly evident in Fig. 3A which shows that the ratio of cross-sectional area of flexor muscle to the area of the abdomen remains constant, as does the ratio of the abdomen/uropod length to cephalothorax length. The amount of area devoted to escape scales as mass to the two-thirds power (Fig. 3B), again consistent with isometric growth.

Movements

A sample tracing from sequential frame analysis (Fig. 4) shows that, in addition to undergoing large linear accelerations, the body of the shrimp also undergoes large rotational motions. Using the position of the body in the first image as a frame of reference, the body rotates through an angle of about 75° and accelerates in both the x- and y-directions at a magnitude greater than $100\,m\,s^{-2}$. The ventral view of the animal shows that the uropods spread out during the flip to form a fan that is twice the width of the body.

The instantaneous speeds of four individuals, all approximately 7 cm long, are summarized in Fig. 5. These data show that tail-flips last approximately 30 ms and result in speeds of about $3{\cdot}0\,m\,s^{-1}$ with mean accelerations of about $150\,m\,s^{-2}$. In such instances, animals will travel about 0·05 m in the duration of tail flexion. Following this powerful movement, speeds of about $2{\cdot}0\,m\,s^{-1}$ lasting 0·1 s will yield a glide of about 0·1 m for a total of 0·15 m travelled for one escape response.

Hydrodynamic coefficients

For a Reynolds number range of 20 000–80 000, there was no significant trend in the drag coefficients for either model. Both models had drag coefficients which, averaged over all flow speeds, were 0·27 (small model, 0·268; large model, 0·272)

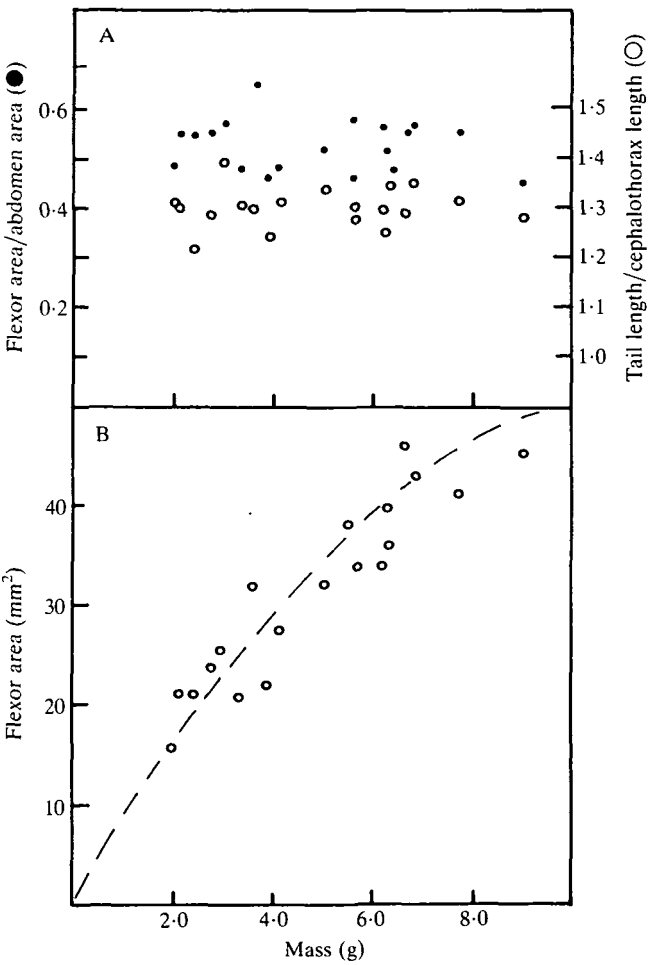

Fig. 3. (A) The ratio of the cross-sectional area of flexor muscle to total cross-sectional area of the abdomen (●) and the ratio of total tail length to cephalothorax length (○) plotted against body mass. (B) A plot of the cross-sectional area of flexor muscle as a function of body mass. These data have a best fit that scales as mass to the 2/3 power ($A = 11{\cdot}76\,m^{0{\cdot}633}$, $r^2 = 0{\cdot}86$, $N = 19$, where A is flexor area in mm^2 and m is the mass of the animal in g).

Therefore, drag coefficients may be treated as constants for escaping shrimps. For the two models, the average added-mass coefficient was 0·4 ($N = 13$, S.E. = 0·09). The central point of these results is that the coefficients do not vary significantly with the size or Reynolds number of the animal. There are two reasons for this lack of variation. First, drag coefficients for objects of similar shape whose Reynolds numbers are greater than about 10000 are fairly constant (Vogel, 1981; Hoerner, 1965). Added-mass coefficients are generally independent of size and acceleration (for few diameters of travel, otherwise see Sarpkaya & Isaacson, 1981) and reflect how the shape of a particular body influences ideal flow patterns

around it (Batchelor, 1967; Daniel, 1984). These data, therefore, confirm classical observations and provide direct numerical values for the analyses that follow. A value of 0·3 for the drag coefficient and 0·4 for the added-mass coefficients are used in the analyses below.

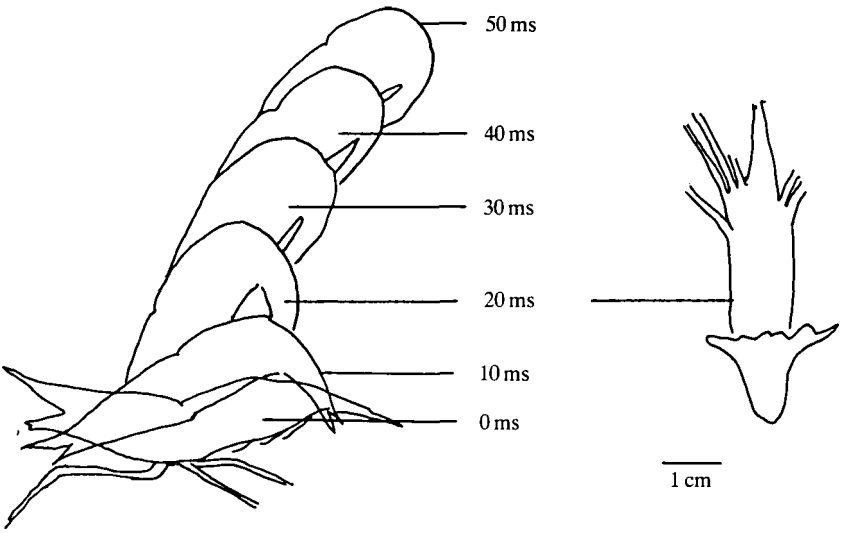

Fig. 4. Sequential film tracings of a 7 cm specimen every 10 ms. This individual undergoes a rotation of nearly 75° with an acceleration of 150 m s^{-2}. To the right is a ventral view of an animal 20 ms after the onset of escape showing the fanning of the uropods.

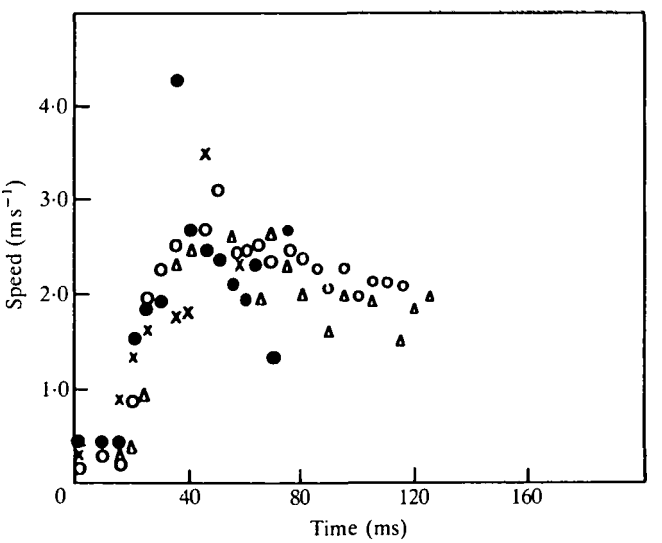

Fig. 5. Speed is plotted against time for four individuals (four different symbols) all about 7 cm in length. These data show that speeds between 2 and 3 m s^{-1} and accelerations in excess of 100 m s^{-2} are common.

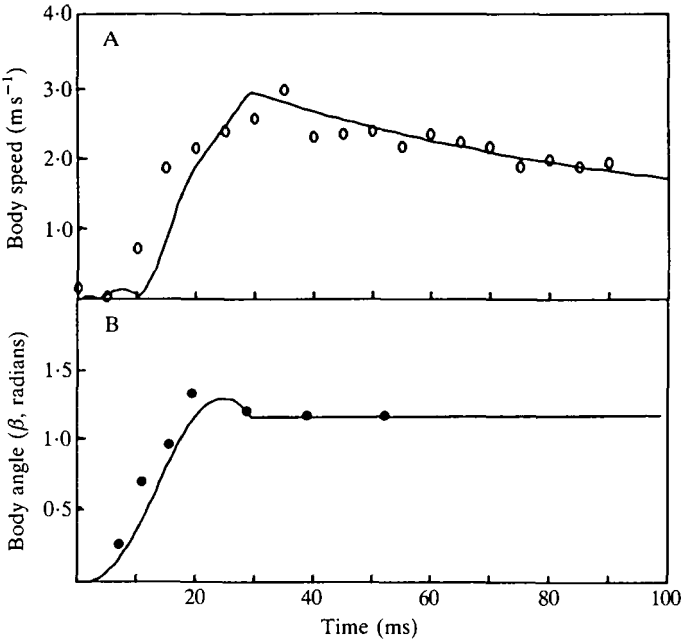

Fig. 6. (A) The open circles from Fig. 5 are plotted against time along with the predicted speed (solid line) of the body. The input parameters used in the simulation are summarized in Table 1. The lower panel is a plot of measured (●) and predicted (solid line) body angles (β) as a function of time.

Theory and experiment: model results

Results from the film analyses show that the body undergoes large accelerations for both rotational and translational motions as a result of a tail-flip that lasts approximately 30 ms. During this event, and the additional 60–70 ms of glide that follows the tail-flip, the animal moves through a distance of about 0·15 m, yielding an average speed of about 1 m s^{-1}. The goal now is to determine the extent to which the theoretical abstraction of this escaping animal can correctly account for these motions.

Direct comparisons

Measured and predicted body speeds and body rotations show excellent agreement (Fig. 6A,B). In general, the theory provides estimates of kinematic parameters that are within 10% of their measured values. The data in Fig. 6, a sample set from Fig. 5, correspond to a shrimp 7 cm in length whose tail-flip lasts 30–35 ms. Additional measured, assumed and predicted parameters are shown in Table 1. Table 1 differentiates between input parameters (assumed) and output parameters (predicted) for the model and shows that predictions for both translational speeds and rotational movements correspond nicely to their measured values.

A further test of the analysis is shown in Fig. 7 in which the predicted angle and

Table 1. *Measured, assumed and predicted parameters corresponding to the motion of a shrimp 7 cm in length*

Parameter	Measured value	Assumed (A) or predicted (P)	
Cephalothorax length	3·5 cm	3·5 cm	(A)
Cephalothorax width	1·7 cm	1·7 cm	(A)
Abdomen length	2·3 cm	2·3 cm	(A)
Abdomen width	1·7 cm	1·7 cm	(A)
Uropod length	1·2 cm	1·2 cm	(A)
Maximum uropod width	3·5 cm	3·5 cm	(A)
Duration of flip	approx. 35 ms	35 ms	(A)
Tail sweep angle	185°	185°	(A)
Drag coefficient	0·3	0·3	(A)
Added-mass coefficient	0·4	0·4	(A)
Maximum body speed	3·1 m s^{-1}	3·05 m s^{-1}	(P)
Maximum body angle (β)	77°	75°	(P)
Distance in 0·1 s	0·16 m	0·135 m	(P)

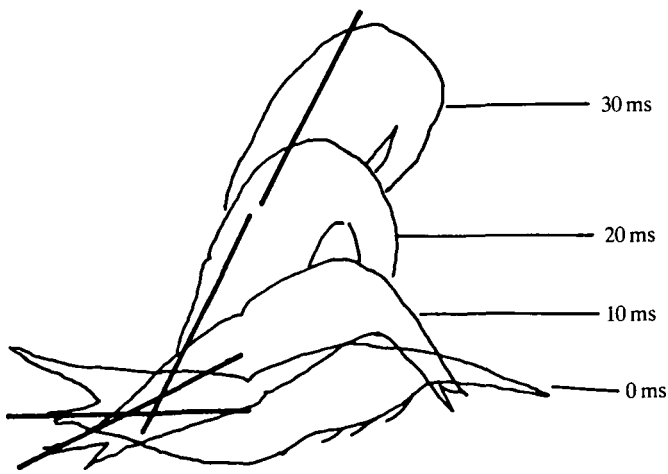

Fig. 7. Sequential film traces along with predicted body motions are superimposed. The solid lines correspond to the predicted motions of the body.

position of the cephalothorax is superimposed upon sequential film traces from Fig. 2. Again, the system of differential equations provides a fairly accurate portrait of the escaping shrimp.

Derived results: magnitudes of thrust forces

In addition to accounting for rotational as well as translational motions, the theory can be used to examine the relative importance of the three different physical mechanisms involved in thrust production for this mode of locomotion

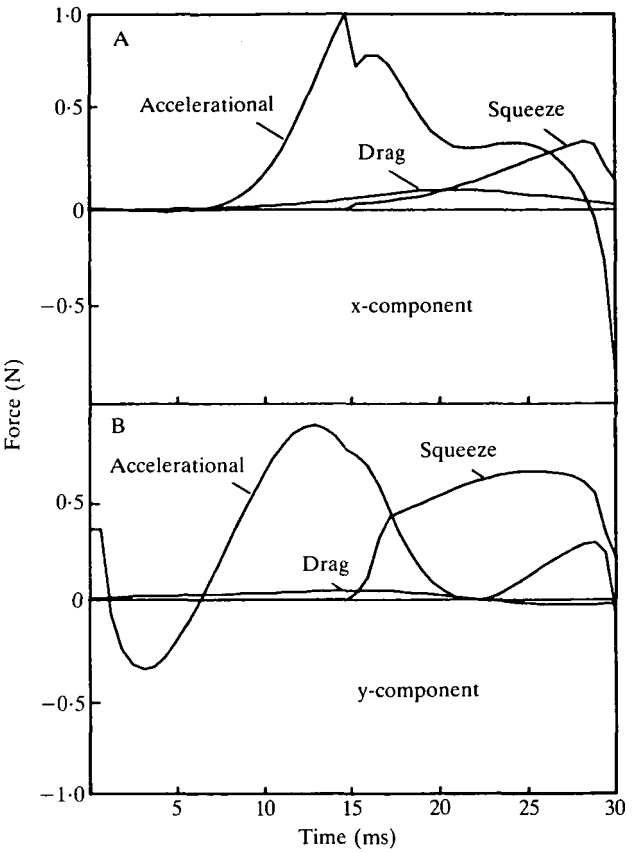

Fig. 8. Predicted forces are plotted against time for both the x-component (A) and the y-component (B) of thrust. The dominant forces, in both cases, arise from the acceleration reaction and the squeeze-force; drag forces are relatively small.

As stated above, thrust is generated by a combination of reactive and resistive forces as well as the force required to squeeze fluid out from the gap subtended by the abdomen and cephalothorax. The latter force is, in general, quite similar to the fling mechanism suggested by Weis-Fogh (1973) and analysed by Lighthill (1973, 1975) for insect flight. Results show that during the early phases of the tail motion, thrust is dominated by reactive forces (Fig. 8). As the speed of the tail increases, resistive forces take an ever greater role in thrust until the point at which squeeze forces begin to dominate. During the last stages of the tail-flip, nearly all the thrust produced arises from the squeeze force. If this force is neglected in the analysis, the theory greatly underestimates the translation of the animal.

Theoretical limitations to performance: scaling and muscle stress

The sum of all forces (x- and y-components) produced during escape divided by the cross-sectional area of muscle yields the total muscle stress required for that

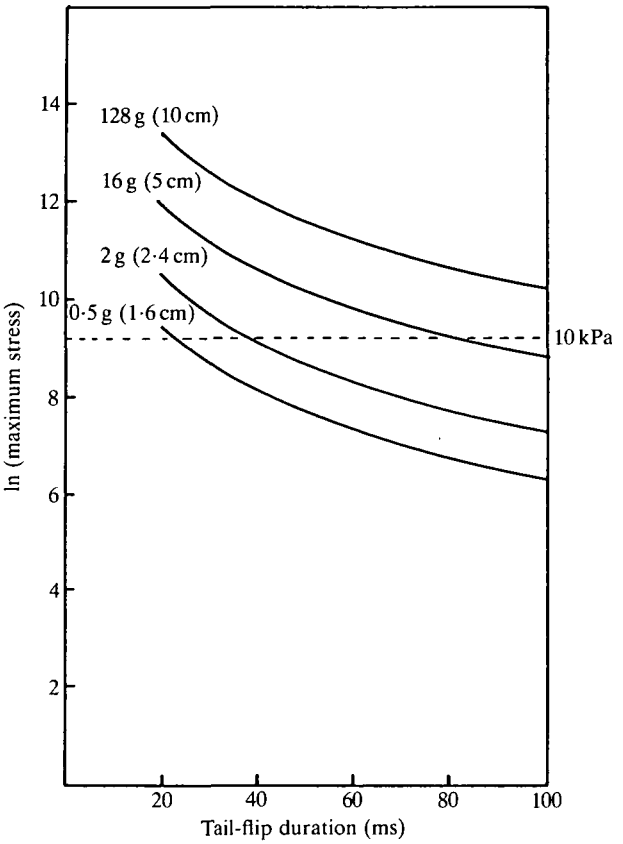

Fig. 9. The natural logarithm of the predicted muscle stress is plotted against tail-flip duration for a variety of sizes, all scaled isometrically. In all cases, the ratio of tail length to cephalothorax length is assumed to be 1·0. The dashed line shows the physiological limit of contractile stress.

movement. The maximum value for this stress occurs at the point during the tail-flip for which thrust forces are greatest, usually towards the end of the flip during the squeeze force. The value of this maximum depends quite strongly on the duration of the tail-flip, and the size of the animal as well as its shape (the ratio of tail to body length, the fineness ratio of the body). Thus, increasing contraction times lead to exponential decreases in the maximum stress (Fig. 9). This decrease arises from the direct relationship between force production and the speed and acceleration of the tail. Similarly, isometric increases in body size also lead to ever greater muscle stresses. Two factors underlie this size dependence. (1) For a given tail-flip duration, greater body sizes yield greater tail speeds and accelerations and, thus, greater forces and stresses. (2) The forces produced during a tail-flip scale, in part, in proportion to the volume of the animal, whereas the stresses scale in proportion to some cross-sectional area. Thus ever greater body sizes will require disproportionately greater stresses.

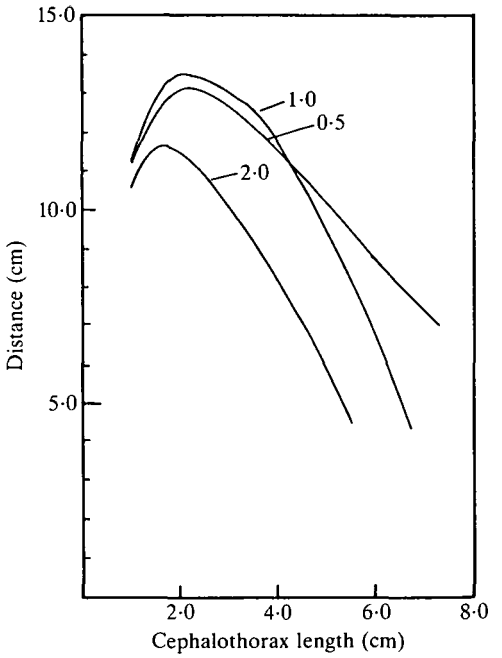

Fig. 10. The total distance travelled in 0·1 s is plotted against body size (cephalothorax length) for three ratios of tail length to cephalothorax length: 0·5, 1·0 and 2·0. An animal with a cephalothorax and tail both 2 cm long translates through the greatest distance.

Presumably, there is some value of stress that cannot be exceeded. For fast-contracting crustacean fibres, the maximum value of propulsive stress should not exceed that generated by the contractile mechanism. Reported values for these stresses vary significantly (see Atwood, 1973; Prosser, 1973), but a reasonable mid-range estimate is about 10 kPa (Atwood, 1973). If stress cannot exceed this value, there appears to be a limitation on both the speed of contraction as well as the size of the animal for any particular shape. This limitation is shown in Fig. 9, in which the dashed line corresponds to the physiological limit of contractile stress.

There are, however, an infinite number of combinations of body sizes and tail-flip durations which yield maximum contractile stresses of 10 kPa. For example, a 2 g shrimp with a 20 ms tail-flip requires the same stress as that of a 16 g shrimp with a 40 ms tail-flip. The physiological limit, therefore, revolves around a trade-off between body size and contraction time. This limit, however, does not in any way directly predict the performance of the animal during escape.

To examine performance in the light of this physiological limit to movement, we took the distance travelled in 0·1 s to be a measure of performance, and monitored those body sizes and flip durations that yielded a maximum stress of 10 kPa. Results of this analysis are summarized in Fig. 10 with a plot of body length *versus* distance travelled during 0·1 s for tail-flip durations requiring 10 kPa of muscle

stress. Note that the results are limited to tail-flips less than or equal to 0·1 s in duration. For those that are less than 0·1 s in duration, the analysis includes the distance covered during a glide phase following the tail-flip. The duration of this glide phase is set so that the total time – glide plus tail-flip duration – is equal to 0·1 s.

Two trends emerge from this analysis. (1) For a particular body shape there is a unique body size that maximizes the total distance travelled, and (2) for a fixed body size, there is a particular ratio of tail length to cephalothorax length that maximizes the total distance travelled. These maxima arise from two factors. First, small bodies have tail-flips of very short duration which still satisfy the condition that 10 kPa of muscle stress is not exceeded. Although such short durations would imply high-speed escapes, the glide phase is comparatively long and the average speed is thus greatly reduced. At the other end of the size spectrum, tail speeds must be quite slow to satisfy the maximum stress condition and, accordingly, body speeds will be quite low.

The second trend, which shows that there is a unique ratio of tail length to body length that maximizes performance, arises from a trade-off between translational and rotational motion. For animals with proportionately small tails, the moments generated by the tail-flip are relatively small and thus the dominant movement is translational. But, because of the small size of the tail, the total thrust that is generated is smaller and translations are, accordingly, smaller as well. As tail length increases relative to body length, both the thrust and moments increase. Eventually, the moments become so large relative to thrust that the body undergoes more rotational than translational movement.

Discussion

Our analysis of the carridean escape manoeuvre considers three issues that pertain to aquatic locomotion in general. First, the fluid-dynamic interaction between the propulsor and the body of an animal leads to a large component of the thrust. Second, our use of a balance of both linear and angular momenta for thrust and resistive forces shows that a trade-off between rotation and translation imposes a limit upon this mode of locomotion. Third, adding an additional constraint, that the total stress in muscles cannot exceed 10 kPa, reveals a size constraint on escape locomotion. Below, we indicate what mechanisms underlie our results and the general implications of these three points.

The squeeze force

The thrust that arises from the fluid-dynamic interaction between the cephalothorax and the abdomen/uropod complex is an important component of the total thrust generated by the rapid tail-flip. As was shown above, neglect of this force leads to a large underestimate of the total thrust and, thus, an incorrect prediction of the trajectory of an escaping shrimp. Thrust generated by this scheme is analogous to the fling mechanism created by the closure of the wings of hovering

insects (Weis-Fogh, 1973; Lighthill, 1973; Ellington, 1984). In this case, as fluid is squeezed out of the region subtended by two wings at the end of a downstroke, large upward forces are generated. The analysis presented in this paper, which incorporates an interaction between the body and propulsor that is analogous to the fling, should apply equally well to the thrust generated by pectoral fins in fishes using labriform locomotion, which have been analysed as drag-based propulsors (Blake, 1981, 1983). For these animals, thrust may be generated by the closure of pectoral fins against the body at the end of the power stroke. Similarly, this squeeze mechanism applies to animals such as dytiscid beetles (Nachtigall, 1980) or other aquatic rowers, in which the closure of paired oar-like appendages should generate thrust by this scheme, possibly of a magnitude far greater than simple drag or inertia-based analyses would predict. Indeed, our analysis shows that the total thrust may be two or three times greater than such analyses would predict.

Rotational versus *translational movement*

Through conservation of both linear and angular momentum, our analysis provides a glimpse of the trade-offs that exist in the design of aquatic organisms for rapid escape manoeuvres. As long as thrust is produced asymmetrically about an animal's centre of gravity, the speeds and trajectories of the body can only be predicted by such an analysis. For example, Weihs's (1972) analysis of fish turning manoeuvres incorporates, in some form, the combined balance of linear and angular momenta to examine turning behaviour. We can conclude from studies of the aero- or hydrodynamics of turning that larger propulsive appendages will yield better turning performance.

The present study, in contrast to analyses of manoeuvrability, shows that larger propulsive appendages do not necessarily lead to better performance. This result follows from a trade-off between total thrust and the total moments generated by thrust. For example, as the length of the abdomen/uropod complex increases, the total thrust generated by movement of that structure clearly increases. Some of the energy from this force goes into translating the body and some goes into rotational movements. As the tail gets longer and longer, ever more thrust is created (as long as flip durations remain constant), but the moment arm of forces about the centre of gravity increases as well. Eventually, the moment arm may become so large that the dominant motion will be rotational. The result is that tails that are greater in length than the body length yield disproportionately more rotation than translation, and performance decays accordingly. Alternatively, tails much smaller in length than the body lead to very little rotation or translation.

Simple isometric increases in body size pose a similar trade-off between rotation and translation. For this case, linear increases in body dimensions lead to nearly cubic increases in thrust, as the hydrodynamic forces scale in part with the area of the abdomen (drag forces) and in part with the volume of the abdomen (acceleration reaction forces). These forces determine the translation of the animal. However, the moments produced by the thrust from the tail increase nearly as the fourth power of the linear dimension of the body. This dependence

arises from the fact that moments are equal to the product of thrust and another linear dimension: the moment arm of thrust about the centre of gravity. Thus, linear increases in size lead to cubic increases in forces that determine translational movements and quartic increases in those determining rotational movements. As bodies become increasingly large, their movements become increasingly dominated by rotational moments.

Predicted stress in flexor muscles

The near cubic rise in thrust with increases in the linear dimension of an animal, as suggested above, would require a rather peculiar situation – the force per cross-sectional area (stress) of abdominal flexors would have to increase as the one-third power of the mass of the animal. We know, however, that the maximum stress produced by contracting muscle is constant for a given muscle type (see for example, Alexander, 1985; McMahon, 1984). A value of 10 kPa is a reasonable estimate of this maximum. Therefore, either absolute or relative changes in the dimensions of the animal must be accompanied by appropriate changes in the speed of tail movement so that this maximum value of stress is never exceeded. For example, an increase in the relative length of the tail must be accompanied by a decrease in the duration of the tail-flip. As was shown above, this physiological constraint upon the motion of shrimps leads to an optimum body size for escape by this mechanism. Moreover, this optimum corresponds with the observed sizes for *Pandalus danae*.

Although imposing the constraint that muscle stress cannot exceed some value leads to a novel prediction for a size limit in escape movements, two problems remain with such an analysis. First, the optimum size we predict falls well below the observed sizes of other decapod crustaceans (e.g. lobsters and crayfish) that use a tail-flip in escape locomotion. For these larger animals, we would expect the relative proportion of flexor cross-sectional area to be greater than is found in the animals used in the present study.

A second issue is that the maximum isometric stress of muscle may not be reached in actual locomotor movements. This issue has recently come into focus with findings of Biewener *et al.* (1988) and Perry *et al.* (1988) that muscle stresses are about one-third of their maximum isometric value during normal locomotion in terrestrial animals. Although the *in situ* stresses have not been measured in *P. danae*, we can suppose that this giant-neurone-mediated escape behaviour maximally excites the flexors, leading to a situation that more closely approaches the maximum isometric condition. Even if the maximum is not reached, the existence of an optimum does not disappear. The value and location of that optimum would, however, decrease slightly with decreasing values for the maximum muscle stress.

Despite the above limitations, our merger of the dynamics of unsteady rotational aquatic locomotion with estimates of the mechanical properties of rapidly contracting flexor muscles provides new insight into the limitations imposed on escape locomotion. These issues are relatively unexplored in studies o

aquatic locomotion. Indeed, most research in this area has, as stated above, emphasized rectilinear steady-state locomotion. Only Wu (1971*a*,*b*,*c*), Weihs (1972), Webb (1983, 1986) and Blake (1983) have considered the problems of either acceleration or turning, and no previous study has considered how these act simultaneously during escape manoeuvres. Even where research has dealt with turning, acceleration or unsteady mechanisms underlying thrust and resistance, the emphasis has been on fish locomotion. Studies of invertebrate, especially arthropod, swimming are few and far between with most attention devoted to steady-state motion (for a review see Hargreaves, 1981). Moreover, it appears that only studies of terrestrial (Taylor, 1985; Alexander, 1985; and in general Taylor *et al.* 1985) and aerial (Ellington, 1984, 1985) locomotion clearly link the physiological or mechanical properties of contracting muscle to the physics of propulsion. In the case of escape locomotion by shrimps, only such combined approaches can give insight into limitations to the performance of the animal.

We thank A. O. D. Willows for providing space and support at the Friday Harbor Laboratories and D. Duggins for help in collecting animals. T. Williams and C. Jordan provided useful comments on the manuscript. Conversations with P. Webb on related topics are greatly appreciated. We also thank the support of the National Science Foundation (grant DCB-8711654).

References

ALEXANDER, R. McN. (1985). The maximum forces exerted by animals. *J. exp. Biol.* **115**, 231–238.

ATWOOD, H. L. (1973). An attempt to account for the diversity of crustacean muscles. *Am. Zool.* **13**, 357–378.

BATCHELOR, G. K. (1967). *An Introduction to Fluid Dynamics.* London: Cambridge University Press.

BIEWENER, A. A., BLICKHAN, R., PERRY, A. K., HEGLUND, N. C. & TAYLOR, C. R. (1988). Muscle forces during locomotion in kangaroo rates: force platform and tendon buckle measurements compared. *J. exp. Biol.* **137**, 191–205.

BLAKE, R. W. (1981). Mechanics of drag-based mechanisms of propulsion in aquatic vertebrates. *Symp. zool. Soc. Lond.* **48**, 29–52.

BLAKE, R. W. (1983). *Fish Locomotion.* London: Cambridge University Press.

BONE, Q. & TRUEMAN, E. R. (1983). Jet propulsion in salps (Tunicata: Thaliacea). *J. Zool., Lond.* **201**, 481–506.

BRENNEN, C. E. (1982). A review of added mass and fluid inertial forces. *Nav. Civ. Eng. Lab. Rep.* no. CR82.010.

DANIEL, T. L. (1983). Mechanics and energetics of medusan jet propulsion. *Can. J. Zool.* **61**, 1406–1420.

DANIEL, T. L. (1984). Unsteady aspects of aquatic locomotion. *Am. Zool.* **24**, 121–134.

DANIEL, T. L. (1985). Cost of locomotion: unsteady medusan swimming. *J. exp. Biol.* **119**, 149–164.

DANIEL, T. L. & WEBB, P. W. (1987). Physical determinants of locomotion. In *Comparative Physiology: Life in Water and on Land* (ed. P. Dejours, L. Bolis, C. R. Taylor & E. R. Weibel), pp. 343–369. Padova: Liviana Press.

DENNY, M. (1982). Forces acting on intertidal organisms due to breaking waves: design and application of a telemetry system. *Limnol. Oceanogr.* **27**, 178–183.

DENNY, M., DANIEL, T. L. & KOEHL, M. A. R. (1985). Mechanical limits to size in wave-swept organisms. *Ecol. Monogr.* **55**, 69–102.

ELLINGTON, C. P. (1984). The aerodynamics of hovering insect flight (I–IV). *Phil. Trans. R. Soc. Ser.* B **305**, 1–181.

ELLINGTON, C. P. (1985). Power and efficiency of insect flight muscle. *J. exp. Biol.* **115**, 293–304.

HARGREAVES, B. R. (1981). Energetics of crustacean swimming. In *Locomotion and Energetics in Arthropods* (ed. C. F. Herreid & C. R. Fourtner). New York: Plenum Press.

HERREID, C. F. & FOURTNER, C. R. (1981). *Locomotion and Energetics in Arthropods*. New York: Plenum Press.

HOERNER, S. F. (1965). *Fluid-Dynamic Drag*. New Jersey: Hoerner Fluid Dynamics.

LIGHTHILL, M. J. (1973). On the Weis-Fogh mechanism of lift generation. *J. Fluid Mech.* **60**, 1–17.

LIGHTHILL, M. J. (1975). *Mathematical Biofluiddynamics*. Philadelphia: Soc. Ind. Appl. Math.

MCMAHON, T. A. (1984). *Muscles, Reflexes, and Locomotion*. New Jersey: Princeton University Press.

MATHEWS, J. H. (1987). *Numerical Methods for Computer Science, Engineering, and Mathematics*. New Jersey: Prentice-Hall.

NACHTIGALL, W. (1980). Mechanics of swimming in water beetles. In *Aspects of Animal Movement* (ed. H. Y. Elder & E. R. Trueman), pp. 107–124. London: Cambridge University Press.

O'DOR, R. K. (1988). The forces acting on a swimming squid. *J. exp. Biol.* **137**, 421–442.

PERRY, A. K., BLICKHAN, R., BIEWENER, A. A., HEGLUND, N. C. & TAYLOR, C. R. (1988). Preferred speeds in terrestrial vertebrates: are they equivalent? *J. exp. Biol.* **137**, 207–219.

PROSSER, C. L. (1973). *Comparative Animal Physiology*. Philadelphia: W. B. Saunders.

SARPKAYA, T. & ISAACSON, M. (1981). *Mechanics of Wave Forces on Offshore Structures*. New York: Van Nostrand Reinhold.

TAYLOR, C. R. (1985). Force development during sustained locomotion: a determinant of gait, speed, and metabolic power. *J. exp. Biol.* **115**, 253–262.

TAYLOR, C. R., WEIBEL, E. & BOLIS, L. (eds) (1985). *Design and Performance of Muscular Systems. J. exp. Biol.* **115**, 1–412.

VOGEL, S. (1981). *Life in Moving Fluids*. New Jersey: Princeton University Press.

WEBB, P. W. (1976). The effect of size on the fast-start performance of rainbow trout (*Salmo gairdneri* Richardson) and a consideration of piscivorous predator–prey interactions. *J. exp. Biol.* **65**, 157–177.

WEBB, P. W. (1979). Mechanics of escape responses in crayfish (*Oronectes virilis* Hagen). *J. exp. Biol.* **79**, 245–263.

WEBB, P. W. (1983). Speed, acceleration and manoeuvrability of two teleost fishes. *J. exp. Biol.* **102**, 115–122.

WEBB, P. W. (1984). Form and function in fish swimming. *Scient. Am.* **251**, 72–82.

WEBB, P. W. (1986). Effect of body form and response threshold on the vulnerability of four species of teleost prey attacted by large-mouth bass (*Micropterus salmoides*). *Can. J. Fish. aquat. Sci.* **43**, 763–771.

WEIHS, D. (1972). A hydrodynamic analysis of fish turning manoeuvres. *Proc. R. Soc.* B **182**, 59–72.

WEIHS, D. (1974). Energetic advantages to burst swimming in fish. *J. theor. Biol.* **48**, 215–229.

WEIHS, D. (1980). Energetic significance of changes in swimming modes during growth of anchovy larvae, *Engraulis mordax*. *Fishery Bull. Fish Wildl. Serv. U.S.* **77**, 597–604.

WEIHS, D. & WEBB, P. W. (1983). Optimization of locomotion. In *Fish Biomechanics* (ed. P. W. Webb & D. Weihs), pp. 339–371. New York: Praeger Press.

WEIS-FOGH, T. (1973). Quick estimates of flight fitness in hovering animals, including novel mechanisms for lift production. *J. exp. Biol.* **59**, 169–230.

WU, T. Y. (1971*a*). Hydromechanics of swimming propulsion. I. Swimming of a two-dimensional flexible plate at variable forward speeds in an inviscid fluid. *J. Fluid Mech.* **46**, 337–355.

WU, T. Y. (1971*b*). Hydromechanics of swimming propulsion. II. Some optimum shape problems. *J. Fluid Mech.* **46**, 521–544.

WU, T. Y. (1971*c*). Hydromechanics of swimming propulsion. III. Swimming of a slender fish with side fins. *J. Fluid Mech.* **46**, 545–568.

Wu, T. Y. (1975). Hydromechanics of fish swimming. In *Swimming and Flying in Nature* (ed. T. Y. Wu, C. J. Brokaw & C. Brennen), pp. 615–634. New York: Plenum Press.
Wu, T. Y., Brokaw, C. J. & Brennen, C. (1975). *Swimming and Flying in Nature*. New York: Plenum Press.
Wylie, C. R. (1975). *Advanced Engineering Mathematics*. New York: McGraw Hill.
Yates, G. T. (1986). Optimum pitching axes of flapping wing propulsion. *J. theor. Biol.* **120**, 255–276.